JCTC Journal of Chemical Theory and Computation

Article

Cite This: J. Chem. Theory Comput. 2019, 15, 3868−3874

pubs.acs.org/JCTC

Thermodynamic Stability of Polar and Nonpolar Amyloid Fibrils

Farbod Mahmoudinobar,[†] Jennifer M. Urban,[‡] Zhaoqian Su,[¶] Bradley L. Nilsson,[‡] and Cristiano L. Dias*[,†]

[†]Department of Physics, New Jersey Institute of Technology, Newark, New Jersey 07102, United States

[‡]Department of Chemistry, University of Rochester, Rochester, New York 14627, United States

[¶]Department of Systems and Computational Biology, Albert Einstein College of Medicine, Bronx, New York 10461, United States

Supporting Information

ABSTRACT: Thermodynamic stabilities of amyloid fibrils remain mostly unknown due to experimental challenges. Here, we combine enhanced sampling methods to simulate all-atom models in explicit water in order to study the stability of nonpolar ($A\beta_{16-21}$) and polar ($IAPP_{28-33}$) fibrils. We find that the nonpolar fibril becomes more stable with increasing temperature, and its stability is dominated by entropy. In contrast, the polar fibril becomes less stable with increasing temperature, while it is stabilized by enthalpy. Our results show that the nature of side chains in the dry core of amyloid fibrils plays a dominant role in accounting for their thermodynamic stability.

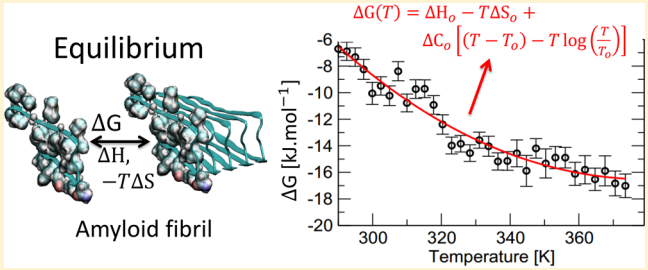

1. INTRODUCTION

Peptide self-assembly into cross-β fibril structures has important implications for plaque formation in amyloid diseases that include Alzheimer's and Parkinson's.[1,2] Accordingly, this phenomenon has been the subject of intensive studies to provide insights into the critical interactions that need to be targeted by drugs to avoid plaque formation. Interactions between backbone atoms, which are common to all peptides, play an important role in accounting for the superior mechanical strength of fibrils,[3,4] and they may explain the universal nature of fibrils that can form from seemingly unrelated amino acid sequences given the right conditions.[5,6] Side chain interactions modulate the rate of fibrillization which increases with the hydrophobicity and the β-sheet propensity of the peptide sequence.[7] These interactions may also play an important role in accounting for the thermodynamic stability of cross-β structures as shown in alanine scanning mutagenesis experiments.[8] In such experiments, the free-energy (ΔG) to add an $A\beta_{1-40}$ peptide to a fibril changed by up to ~2 kcal/mol when a single residue was mutated to alanine. It is important to note that equivalent ΔG values can emerge from different combinations of enthalpy (ΔH) and entropic energy ($-T\Delta S$), i.e., $\Delta G = \Delta H - T\Delta S$. Knowledge of ΔH and $-T\Delta S$ can provide insights into the stabilizing mechanisms of fibrils since hydrophobic interactions of small nonpolar side chains are mainly related to ΔS, whereas ΔH emerges mainly from direct pairwise interactions, e.g., van der Waals and electrostatic interactions.[9−11] Thus, thermodynamics provides a framework to quantify fibril stability and the interactions accounting for it.

Albeit commonly used to study protein folding, equilibrium thermodynamic quantities of mature amyloid fibrils are not easily accessible experimentally, and they remain largely unknown.[12−14] Only recently have experiments shown that for some protein sequences, fibrils grow to an equilibrium state in which they coexist with dissolved proteins.[15] The threshold concentration of proteins dissolved in solution below which fibril nucleation cannot occur[16] has been explored to measure ΔG and to discover effects of individual amino acids on the stability of fibrils.[17−20] Studies of the temperature dependence of this equilibrium can also be used to compute other thermodynamic quantities, e.g., ΔH, ΔS, and changes in heat capacity ΔC_p.[12,21−23] Studies of β-sheet association provide evidence that the molecular mechanisms accounting for fibril stability depends on the peptide sequence.[24−26] In particular, the enthalpically unfavorable desolvation of preformed β-sheets made from polar peptides (Sup35) could be the rate limiting process of their association, whereas entropic effects related to hydrophobic interactions could favor the association of β-sheets made from nonpolar peptides. It is important to note that while effects of temperature on ΔG are not well understood, higher temperatures have been shown to affect the kinetics of some amyloid fibrils by significantly increasing their nucleation and growth rates.[27]

The spontaneous addition of peptides to fibrils has been studied through computer simulations. This process was shown to occur in at least two steps wherein peptides dock into fibrils before locking into them via nonspecific hydrogen bonds.[23,28−34] To compute ΔG, different simulation setups based on the dissociation of peptides from known fibril structures have been used.[23,35−37] Extensive sampling is required to account for equilibrium ΔG where $\Delta G \equiv$

Received: February 13, 2019
Published: April 30, 2019

DOI: 10.1021/acs.jctc.9b00145
J. Chem. Theory Comput. 2019, 15, 3868−3874

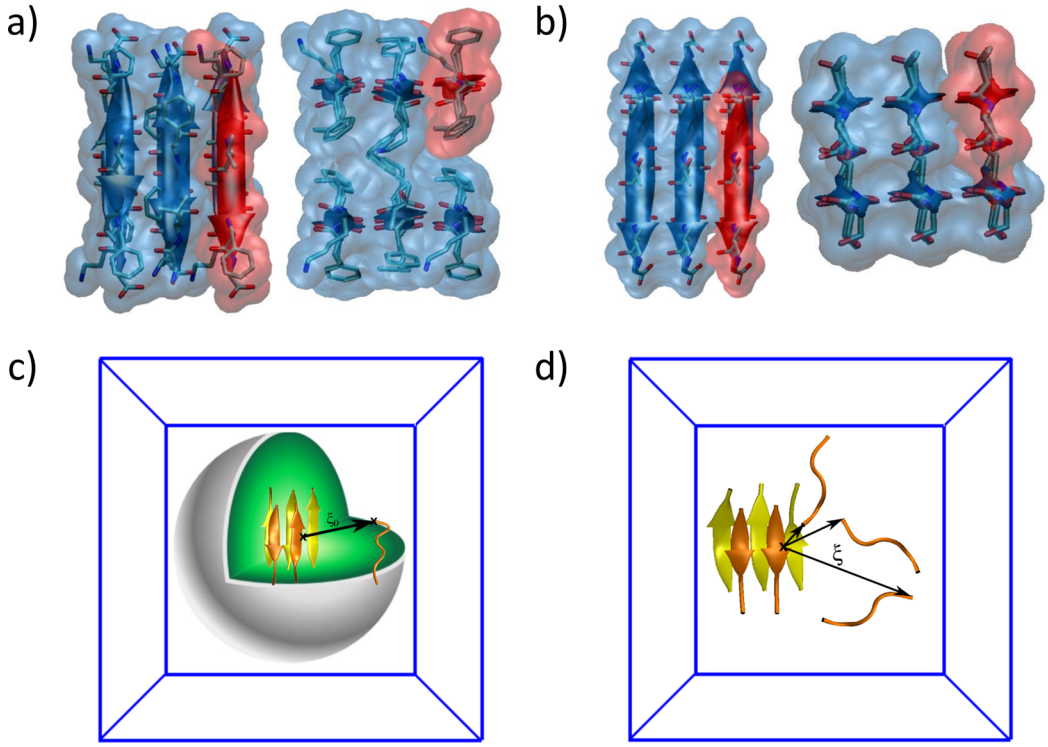

Figure 1. Different views of (a) the antiparallel Aβ_{16-21} and (b) the parallel IAPP$_{28-33}$ fibrils. van der Waals surfaces of the fibril and the free peptide are shown in blue and red, respectively. Residues forming the dry core of Aβ_{16-21} (F and L) and IAPP$_{28-33}$ (S and N) fibrils are highlighted. Schematic representations of the simulation setup showing the reaction coordinate ξ for (c) Aβ_{16-21} and (d) IAPP$_{28-33}$ fibrils. A sphere of radius ξ is shown to highlight the three-dimensional surface (gray) on which the free peptide can move around the Aβ_{16-21} fibril. The initial conformation of the free peptide is shown at three different ξ-values for the IAPP$_{28-33}$ fibril. The two β-sheets accounting for the fibril are shown in yellow and orange. Water molecules are not shown for clarity.

$-\Delta G_{\text{dissociation}} = \Delta G_{\text{association}}$. Recently, ΔG values computed from simulations have been shown to be in reasonable agreement with experiments for the Aβ_{9-40} fibril.[38] These ΔG emerge from a favorable entropic contribution and a small nonfavorable enthalpy. Rationalization of these results requires an understanding of how the amino acid sequence and fibril structure account for equilibrium thermodynamic quantities.

In this paper, we compute potentials of mean force (PMF) to add monomeric peptides to nonpolar and polar fibrils. PMF(ξ) corresponds to the free-energy to bring a peptide from noninteracting distances to a distance ξ from the fibril. This quantity is computed at different temperatures in order to provide estimates for ΔH and $-T\Delta S$. Simulations are performed by combining two enhanced sampling methods, i.e., Replica Exchange Molecular Dynamics (REMD) and Umbrella Sampling (US). REMD is used to improve sampling of the different US windows, thus, providing equilibrium ensembles of peptide structures around the fibril at different temperatures. The weighted histogram analysis method (WHAM) is used to compute PMF(ξ) at different temperatures from the different ensembles. We anticipate that the methodology used here will become popular as the intensive computational resources required to perform the simulations are becoming more widely available to researchers. The combination of REMD and umbrella sampling presents the advantage of being easily generalized to other systems as it requires little prior knowledge of the system being study, and it provides equilibrium conformational ensembles at different temperatures.

We find that the nonpolar fibril studied in this paper becomes more stable with increasing temperature. At first sight, this result is counterintuitive as solid materials tend to become less stable with increasing temperature and not the opposite. We show that hydrophobic interactions in the core of nonpolar fibrils are responsible for this nonconventional dependence of stability on temperature. In contrast, the polar fibril becomes less stable with increasing temperature. Thus, our results suggest that the stability of fibrils can be tuned by carefully choosing the amino acid sequence in the dry core of the fibril. Accordingly, one may envisage fibrils being used as thermosensors that will fall apart whenever a given temperature T_c is reached. To the best of our knowledge, this is the first computational study to investigate the effect of temperature on the thermodynamic stability of amyloid-like fibrils using all-atom molecules and explicit solvent. Moreover, the combination of REMD and US allows us to compute enthalpic and entropic energies with small uncertainties for both nonpolar and polar fibrils. We find that the former is stabilized by entropic energy, and the latter is stabilized by enthalpy. This suggests, that similarly to the thermodynamic theory of protein folding, it may be possible to develop a thermodynamic theory for fibril growth wherein the addition of a peptide to a fibril accounts for specific changes in enthalpy, entropic energy, and heat capacity. However, this will require the study of other fibrils from different amino acid sequences as well as polymorphic fibril structures. This study provides a proof of concept in that direction and shows a new methodology that can be used for that purpose.

DOI: 10.1021/acs.jctc.9b00145
J. Chem. Theory Comput. 2019, 15, 3868−3874

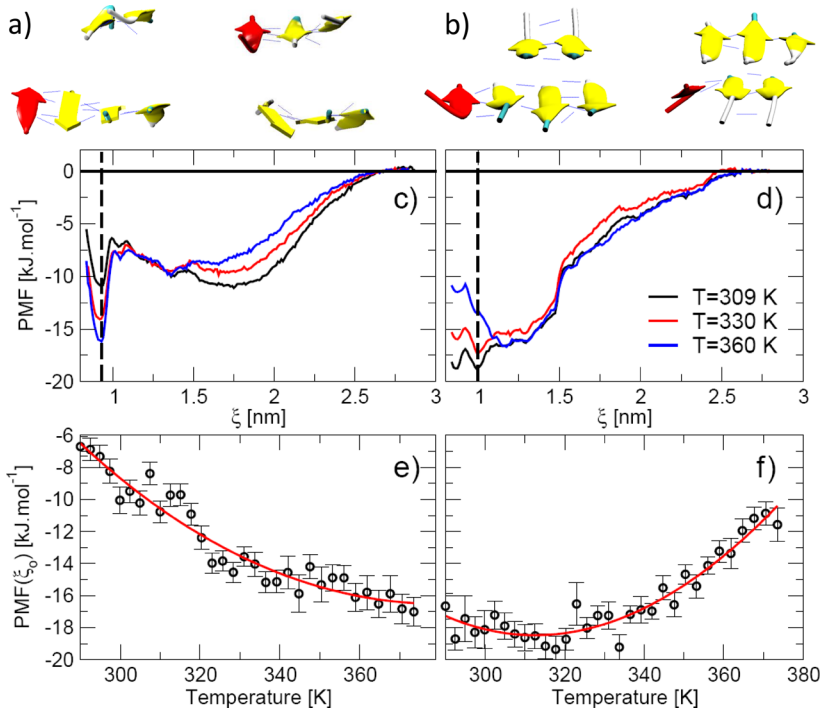

Figure 2. Characteristic configurations of the peptide (in red) locked into (a) Aβ_{16-21} and (b) IAPP$_{28-33}$ fibrils. Backbone hydrogen bonds are represented by dotted blue lines, and β-sheet structures in the fibril are represented in yellow. PMF to add a peptide to the fibril along the reaction coordinate ξ for (c) Aβ_{16-21} and (d) IAPP$_{28-33}$ fibrils at 309 K (black), 330 K (red), and 360 K (blue). Temperature dependence of the PMF at locked state for (e) Aβ_{16-21} and (f) IAPP$_{28-33}$ fibrils. Red lines correspond to fits of the PMF at ξ_0 to eq 1, and error bars were computed using bootstrap analysis.

2. METHODS

All simulations are performed using GROMACS 4.6 with AMBER99sb-ILDN force-field and TIP3P water.[39] The initial structure of the nonpolar Aβ_{16-21} fibril (sequence KLVFFA) is based on the PDB entry 3OW9 which contains 12 antiparallel peptides.[40] To reduce the computational cost of the simulation while allowing the free peptide to interact with the solvent accessible sides of the fibril, we retain six of the 12 peptides in the simulation box—see Figure 1a. The polar IAPP$_{28-33}$ fibril (sequence SSTNVG) was constructed by extending the PDB entry 3DG1[71] to account for a cross-β structure made of six chains with parallel β-sheets as determined experimentally[41,42]—see Figure 1b. Simulation boxes of Aβ_{16-21} and IAPP$_{28-33}$ fibrils are solvated with 7379 and 7300 water molecules, and the net charge of the Aβ_{16-21} system is neutralized by adding six Cl^- ions. These initial fibrils were relaxed for 2 ns at 300 K and 1 atm to remove unrealistic contacts. Details of the simulation protocol are given in the Supporting Information (SI).[71]

A two-step Umbrella Sampling protocol[36] combined with replica exchange molecular dynamics is used to study fibril dissociation at different temperatures. Notice that US (without REMD) is commonly used to study free-energies to add peptides to a fixed-main chain fibril.[37,38,43−45] The combination of US and REMD enhances sampling of the phase space (see section S6 of the SI[71]), and it provides estimates of the PMF at different temperatures which we use to compute enthalpy and entropic energy. In these simulations, heavy atoms of five chains of the initial fibril are restrained to their initial positions by a spring with constant 1000 kJ mol^{-1} nm^{-2}.

In the first US step, the C_α atom of the N-terminal of the "free" peptide is pulled away from the center-of-mass of its closest three chains along the one-dimensional direction of the fibril axis (ξ_z). From these 10 ns steered molecular dynamics simulations, 20 and 19 configurations for Aβ_{16-21} and IAPP$_{28-33}$, respectively, were extracted along the dissociation pathway. The ξ_z distance between peptide and fibril in these extracted configurations was in the range of 0.9−2.8 nm for Aβ_{16-21} and 0.94−2.74 nm for IAPP$_{28-33}$ with 0.1 nm increments for both systems. The goal is to use these structures as initial configurations to sample the system along the reaction coordinate.

We define the distance ξ between the C_α atom of the N-terminal of the "free" peptide and the center-of-mass of the three closest chains of the fibril as our reaction coordinate for the second step of umbrella sampling—see the SI.[71] The selection of ξ in this way limits the conformations of the free peptide to move on a sphere with radius ξ at each window—see Figure 1c. To avoid potential biases introduced by the initial structure of the "free" peptide, we removed all the water from the simulation box and performed a manual random rotation of the peptide around its C_α atom of the N-terminal residue, avoiding steric collisions with the fibril. This rotation was performed once for each window of both systems while keeping the distance ξ fixed. Examples of rotations for three ξ values are shown in Figure 1d. The configurations with rotated free peptide were solvated and equilibrated for 2 ns with position restraints on heavy atoms.

In the second US step, a spring with a constant of 4000 kJ mol^{-1} nm^{-2} is used to restrain initial ξ distances of the 20 Aβ_{16-21} and 19 IAPP$_{28-33}$ windows. These systems are simulated using REMD[46] for 75 ns each. The last 25 ns of the trajectories is used to compute PMF(ξ) at each of the 32 temperatures (ranging from 290 to 373 K) using the weighted

DOI: 10.1021/acs.jctc.9b00145
J. Chem. Theory Comput. 2019, 15, 3868−3874

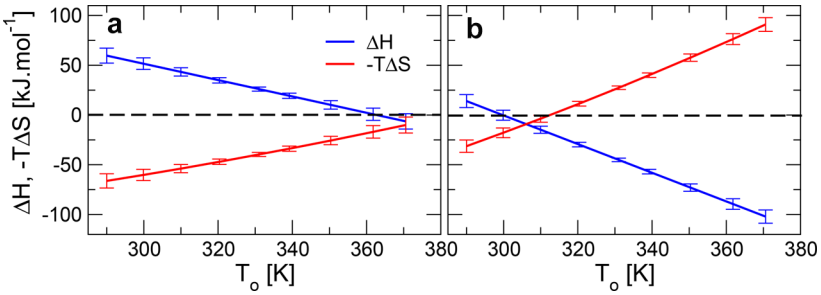

Figure 3. Temperature dependence of the enthalpy ΔH_0 and entropic energy $-T_0\Delta S_0$ for (a) Aβ_{16-21} and (b) IAPP$_{28-33}$ fibrils computed at ξ_0. These quantities were obtained by fitting the PMF to eq 1 at different reference temperatures T_0. Error bars in these figures were obtained from fits to eq 1—see SI.[71]

histogram analysis method.[47] Details of the simulation and analysis of the convergence of the PMF are provided in the Supporting Information (SI).[71] Notice that the PMF increases with $-k_bT\log(\xi^2)$ due to the three-dimensional nature of ξ. We subtract this dependence of the PMF on ξ, and the PMF is shifted to zero at ξ = 2.7 nm.

3. RESULTS

In Figure 2c-d we depict the PMF of Aβ_{16-21} and IAPP$_{28-33}$ fibrils along the reaction coordinate ξ at temperatures 309, 330, and 360 K in black, red, and blue colors, respectively. Global minima of these PMF (dashed lines in Figure 2c-d) correspond to configurations in which the free peptide is locked to the fibril, i.e., the free peptide adopts a β-strand structure that is hydrogen bonded to the fibril. Cluster analysis (see Figure S4 in the SI[71]) shows that locked states are accounted for by two main structures: one where β-sheets are made of four and two peptides (Figure 2a), and the other where both β-sheets of the fibril are made of three peptides each (Figure 2b). The latter structure represents an "ideal fibril" where the peptide is hydrogen bonded to one β-sheet of the fibril and its side chains interact with the opposing β-sheet. Locked structures make up ~70% of the conformations sampled by the peptide at ξ_0 = 0.94 nm for Aβ_{16-21} and ξ_0 = 1.00 nm for IAPP$_{28-33}$. At large distances (ξ > 2.5 nm), the peptide does not interact with the fibril.

The temperature dependence of the PMF at ξ_0, i.e., the locked state, is shown in panels e and f of Figure 2 for Aβ_{16-21} and IAPP$_{28-33}$ fibrils, respectively. These panels show that the nonpolar fibril becomes more stable with increasing temperature, while the opposite is observed for the polar fibril. At first sight, the temperature dependence of the Aβ_{16-21} fibril appears counterintuitive as thermal fluctuations reduce the stability of conventional material. However, this behavior is consistent with hydrophobic interactions becoming stronger with increasing temperature.[48,49] In section S8 of the SI, we discuss how the positively charged lysine in Aβ_{16-21} interacts with the fibril.[71] Further insights into the role of hydrophobic interactions can be obtained by decomposing the PMF into enthalpy $\Delta H_0(\xi)$ and entropic energy $-T_0\Delta S_0(\xi)$ at the reference temperature T_0. These quantities, as well as the heat capacity $\Delta C_{po}(\xi)$ to add a peptide to a fibril, can be obtained by fitting the temperature dependence of the PMF to[50−54]

$$\mathrm{PMF}(\xi, T) = \Delta H_0(\xi) - T\Delta S_0(\xi) + \Delta C_{po}(\xi)\left[(T - T_0) - T\log\left(\frac{T}{T_0}\right)\right] \quad (1)$$

Lines in Figure 2e-f correspond to fits of the PMF at ξ_0 to eq 1. These fits provide a good description of our simulation data as well as numerical estimates for $\Delta H_0(\xi_0)$, $-T\Delta S_0(\xi_0)$, and $\Delta C_{po}(\xi_0)$—see Tables S1 and S2 of the SI.[71] The temperature dependence of $\Delta H_0(\xi_0)$ and $-T_0\Delta S_0(\xi_0)$ is shown in Figure 3. For the Aβ_{16-21} fibril, $-T_0\Delta S_0(\xi_0)$ favors the fibrillar state, while $\Delta H_0(\xi_0)$ opposes it at all temperatures, including physiological conditions, i.e., 310 K. The dominant $-T_0\Delta S_0$ arises from hydrophobic interactions in the core of Aβ_{16-21}.[9,55−57] These interactions emerge because water in the vicinity of nonpolar residues is released into the bulk solution with increased entropy when nonpolar molecules approach each other. The stability of the IAPP$_{28-33}$ fibril is favored by enthalpy, while it is opposed by entropy at temperatures above 306 K. Direct interactions involving atoms of peptide, fibril, and water molecules can rationalize this enthalpic stabilization.[9] The configurational entropy of the peptide which becomes smaller when it binds to the fibril may explain the unfavorable entropic energy of binding of IAPP$_{28-33}$. At physiological conditions, the entropic component is negligible, and the stability of IAPP$_{28-33}$ is dominated by enthalpy.

ΔC_{po} measures the curvature of the temperature dependence of the PMF—see eq 1. For protein folding, this quantity is invariably negative, and it has been related to the burial of nonpolar residues away from water.[49,58,59] Accordingly, ΔC_{po} for protein folding is often written as the sum of negative and positive terms accounting for the desolvation of nonpolar $\Delta C_{po}^{nonpolar}$ and polar ΔC_{po}^{polar} residues, respectively.[58] In contrast to this decomposition, a recent study reported ΔC_{po}^{polar} to be negative for a large class of polar compounds,[60] while experimental studies have called for a re-evaluation of the additive interpretation of ΔC_{po}.[61,62] Amyloid fibrils may constitute ideal systems to study these questions as the hydropathy of their dry core can be tuned by varying the peptide sequence. In our simulations, we find that ΔC_{po} is negative for both Aβ_{16-21} (ΔC_{po} = −0.85 kJ/mol/K) and IAPP$_{28-33}$ (−1.44 kJ/mol/K) fibrils—see Tables S1 and S2.[71] This suggests that the burial into the fibril core of both nonpolar side chains of Aβ_{16-21} and polar side chains of IAPP$_{28-33}$ account for a negative change in heat capacity. However, simulations of other polar fibrils are needed to validate these results.

The lowest temperature probed by our simulations is 290 K. However, eq 1 can be used to extrapolate PMF(ξ_0) to lower temperatures. In particular, the extrapolated PMF(ξ_0) at 265.4 K for Aβ_{16-21} and 227.1 K for IAPP$_{28-33}$ is zero implying that fibrils become unstable at these temperatures. We anticipate

DOI: 10.1021/acs.jctc.9b00145
J. Chem. Theory Comput. 2019, 15, 3868−3874

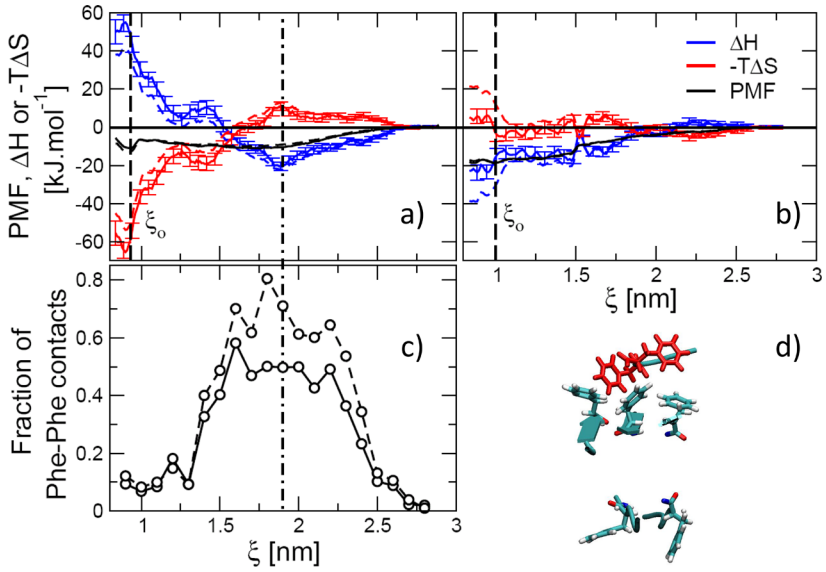

Figure 4. Changes in enthalpy ΔH and entropic energy $-T\Delta S$ as a function of ξ for (a) Aβ_{16-21} and (b) IAPP$_{28-33}$ fibrils at 310 K (full lines) and 320 K (dashed lines). Error bars in these figures are obtained from fits to eq 1. (c) Fraction of contacts between phenylalanine residues of the free-peptide and the fibril at 310 K (full line) and 320 K (dashed line). Residues are considered to be in contact whenever their atoms are at a distance smaller than 0.25 nm from each other. (d) Characteristic configuration of fibril (cyan) and peptide (red) at ξ = 1.8 nm.

that experimental studies of amyloid fibrils at high pressure and/or in solutions containing cosolvents may be used to explore the dissociation of nonpolar fibrils at temperatures below 273 K. Pressure and cosolvents account for a reduction in the freezing point of water, enabling studies at temperatures below 273 K.[53] Experimental evidence that fibrils can dissociate at low temperatures has been provided for α-synuclein.[63−65]

Figure 4 depicts thermodynamic quantities computed along the reaction coordinate, ξ, for Aβ_{16-21} and IAPP$_{28-33}$ fibrils at 310 and 320 K. Panel (a) in Figure 4 shows that the first and second minima of the PMF of the Aβ_{16-21} fibril are favored by entropy and enthalpy, respectively. At the first minimum, nonpolar surfaces of L_{17} and F_{19} side chains are buried in the fibril core (see Figure 1c) accounting for the release of shell water into the bulk and the dominant entropic component of the free-energy. At the second minimum, the peptide interacts with the side of the fibril, maximizing the number of van der Waals and electrostatic interactions, thus explaining the dominance of the enthalpic component. Accordingly, Figure 4c shows that the number of contacts between phenylalanine side chains of the peptide and the fibril is a maximum at the second minimum. A sample conformation in which phenylalanine side chains of the peptide and the fibril are in contact is shown in Figure 4d. In contrast, the dry core of IAPP$_{28-33}$ at locked states is made of polar residues (see Figure 1d) that form electrostatic, van der Waals, and hydrogen bonds with the fibril, accounting for the enthalpically dominant component of the PMF. Accordingly, in Figure S12[71] we show that residue N_{31} of the peptide forms hydrogen bonds with residues N_{31} and S_{29} of the fibril contributing to intra- and inter-β-sheet stability. Notice that the magnitudes of $\Delta H(\xi)$ and $-T\Delta S(\xi)$ in Figure 4a-b are 2−4 times larger than the magnitude of the PMF(ξ). However, since one of these quantities is negative and the other is positive, i.e., enthalpy and entropic energy compensate each other, the magnitude of the PMF is only of the order of 15−20 kJ mol^{-1}.[66]

4. CONCLUSION AND DISCUSSION

In summary, our results support the idea that the molecular mechanisms stabilizing cross-β structures are strongly related to the amino acids that are buried in the fibril core. This is in line with scanning mutagenesis experiments in which ΔG is shown to depend significantly on individual residues that are being mutated,[8,36] bioinformatics estimates of ΔG based on structural complementarity of side chains forming the β-sheet,[67] thermodynamic efforts to design new amino acid sequences that form fibrils,[18−20] and thermodynamic studies of coarse-grained models.[68,69] We find that nonpolar fibrils are stabilized by entropy and destabilized by enthalpy, while the opposite trend is observed for polar fibrils. This suggests that nonpolar fibrils are stabilized by hydrophobic interactions, which are characterized by an increase in the entropy of water molecules, whereas the stability of polar fibrils emerges from van der Waals and electrostatic bonds including hydrogen bonds. Notice that in implicit water simulations, enthalpy and entropy were found to contribute equally to the free-energy of a nonpolar fibril[70] suggesting that an explicit treatment of water may be required to account for thermodynamic properties.

Limitations of the present work should also be noted. In particular, our simulations are based on fibril models with fixed main-chains. They provide a template that corresponds to a deep free-energy minimum of the system as the peptide is found locked to the fibril in approximately 70% of the time for small ξ distances. However, more relaxed conformational restrictions of the fibril will be necessary to explore, for example, conformational fluctuations at the fibril end and how it affects transient states leading to the locked state.[45] Also, it is desirable to reproduce results from this work with different force-fields. The extensive computational resources required to simulate 48 μs for Aβ_{16-21} and 45.6 μs for IAPP$_{28-33}$ in boxes containing ∼7,300 water molecules have so far prevented us from doing so. However, strengthening of hydrophobic interactions and weakening of direct interactions with increasing temperature, which gives rise to the entropic and

DOI: 10.1021/acs.jctc.9b00145
J. Chem. Theory Comput. 2019, 15, 3868−3874

enthalpic stability of nonpolar and polar fibrils, are robustly reproduced by different force-fields. This provides evidence that qualitative results from this work are independent of the force-field.

■ ASSOCIATED CONTENT

Supporting Information

The Supporting Information is available free of charge on the ACS Publications website at DOI: 10.1021/acs.jctc.9b00145.

Figures S0−S12 showing details of simulations, REMD overlap and convergence, reaction coordinate details and cluster analysis, structural quantities, effect of temperature on calculated thermodynamic parameters, comparison of MD simulations with and without replica-exchange, error analysis, side chain interaction analysis for LYS and ASN (PDF)

■ AUTHOR INFORMATION

Corresponding Author

*E-mail: cld@njit.edu.

ORCID

Farbod Mahmoudinobar: 0000-0002-4647-598X
Jennifer M. Urban: 0000-0002-8987-5991
Bradley L. Nilsson: 0000-0003-1193-3693
Cristiano L. Dias: 0000-0002-8765-3922

Notes

The authors declare no competing financial interest.

■ REFERENCES

(1) Dobson, C. M. Protein Folding and Misfolding. *Nature* **2003**, *426*, 884−890.
(2) Chiti, F.; Dobson, C. M. Protein Misfolding, Functional Amyloid, and Human Disease. *Annu. Rev. Biochem.* **2006**, *75*, 333−366.
(3) Knowles, T. P.; Fitzpatrick, A. W.; Meehan, S.; Mott, H. R.; Vendruscolo, M.; Dobson, C. M.; Welland, M. E. Role of intermolecular forces in defining material properties of protein nanofibrils. *Science* **2007**, *318*, 1900−1903.
(4) Keten, S.; Xu, Z.; Ihle, B.; Buehler, M. J. Nanoconfinement controls stiffness, strength and mechanical toughness of β-sheet crystals in silk. *Nat. Mater.* **2010**, *9*, 359−367.
(5) Fändrich, M.; Fletcher, M. A.; Dobson, C. M. Amyloid Fibrils from Muscle Myoglobin. *Nature* **2001**, *410*, 165−166.
(6) Fändrich, M.; Dobson, M. Christopher The Behaviour of Polyamino Acids Reveals an Inverse Side Chain Effect in Amyloid Structure Formation. *EMBO J.* **2002**, *21*, 5682−5690.
(7) Chiti, F.; Stefani, M.; Taddei, N.; Ramponi, G.; Dobson, C. M. Rationalization of the effects of mutations on peptide andprotein aggregation rates. *Nature* **2003**, *424*, 805−808.
(8) Williams, A. D.; Shivaprasad, S.; Wetzel, R. Alanine Scanning Mutagenesis of Aβ(1−40) Amyloid Fibril Stability. *J. Mol. Biol.* **2006**, *357*, 1283−1294.
(9) Chaires, J. B. Calorimetry and thermodynamics in drug design. *Annu. Rev. Biophys.* **2008**, *37*, 135−151.
(10) Ladbury, J. E. Calorimetry as a tool for understanding biomolecular interactions and an aid to drug design. *Biochem. Soc. Trans.* **2010**, *38*, 888−893.
(11) Zangi, R. Driving force for hydrophobic interaction at different length scales. *J. Phys. Chem. B* **2011**, *115*, 2303−2311.
(12) Ikenoue, T.; Lee, Y.-H.; Kardos, J.; Yagi, H.; Ikegami, T.; Naiki, H.; Goto, Y. Heat of supersaturation-limited amyloid burst directly monitored by isothermal titration calorimetry. *Proc. Natl. Acad. Sci. U. S. A.* **2014**, *111*, 6654−6659.
(13) Doyle, C. M.; Rumfeldt, J. A.; Broom, H. R.; Broom, A.; Stathopulos, P. B.; Vassall, K. A.; Almey, J. J.; Meiering, E. M. Energetics of oligomeric protein folding and association. *Arch. Biochem. Biophys.* **2013**, *531*, 44−64.
(14) Morel, B.; Varela, L.; Conejero-Lara, F. The Thermodynamic Stability of Amyloid Fibrils Studied by Differential Scanning Calorimetry. *J. Phys. Chem. B* **2010**, *114*, 4010−4019.
(15) O'Nuallain, B.; Shivaprasad, S.; Kheterpal, I.; Wetzel, R. Thermodynamics of A$_\beta$(1−40) Amyloid Fibril Elongation. *Biochemistry* **2005**, *44*, 12709−12718.
(16) Kashchiev, D.; Cabriolu, R.; Auer, S. Confounding the paradigm: peculiarities of amyloid fibril nucleation. *J. Am. Chem. Soc.* **2013**, *135*, 1531−1539.
(17) Wetzel, R. Kinetics and Thermodynamics of Amyloid Fibril Assembly. *Acc. Chem. Res.* **2006**, *39*, 671−679.
(18) Doran, T. M.; Kamens, A. J.; Byrnes, N. K.; Nilsson, B. L. Role of amino acid hydrophobicity, aromaticity, and molecular volume on IAPP (20−29) amyloid self-assembly. *Proteins: Struct., Funct., Genet.* **2012**, *80*, 1053−1065.
(19) Senguen, F. T.; Lee, N. R.; Gu, X.; Ryan, D. M.; Doran, T. M.; Anderson, E. A.; Nilsson, B. L. Probing aromatic, hydrophobic, and steric effects on the self-assembly of an amyloid-β fragment peptide. *Mol. BioSyst.* **2011**, *7*, 486−496.
(20) Senguen, F. T.; Doran, T. M.; Anderson, E. A.; Nilsson, B. L. Clarifying the influence of core amino acid hydrophobicity, secondary structure propensity, and molecular volume on amyloid-β 16−22 self-assembly. *Mol. BioSyst.* **2011**, *7*, 497−510.
(21) Chang, W. E.; Takeda, T.; Raman, E. P.; Klimov, D. K. Molecular dynamics simulations of anti-aggregation effect of ibuprofen. *Biophys. J.* **2010**, *98*, 2662−2670.
(22) Urbic, T.; Najem, S.; Dias, C. L. Thermodynamic properties of amyloid fibrils in equilibrium. *Biophys. Chem.* **2017**, *231*, 155−160.
(23) Takeda, T.; Klimov, D. K. Replica Exchange Simulations of the Thermodynamics of Aβ Fibril Growth. *Biophys. J.* **2009**, *96*, 442−452.
(24) Thirumalai, D.; Reddy, G.; Straub, J. E. Role of Water in Protein Aggregation and Amyloid Polymorphism. *Acc. Chem. Res.* **2012**, *45*, 83−92.
(25) Krone, M. G.; Hua, L.; Soto, P.; Zhou, R.; Berne, B. J.; Shea, J.-E. Role of Water in Mediating the Assembly of Alzheimer Amyloid-β Aβ16−22 Protofilaments. *J. Am. Chem. Soc.* **2008**, *130*, 11066−11072.
(26) Reddy, G.; Straub, J. E.; Thirumalai, D. Dry amyloid fibril assembly in a yeast prion peptide is mediated by long-lived structures containing water wires. *Proc. Natl. Acad. Sci. U. S. A.* **2010**, *107*, 21459−21464.
(27) Uversky, V. N.; Li, J.; Fink, A. L. Evidence for a Partially Folded Intermediate in α-Synuclein Fibril Formation. *J. Biol. Chem.* **2001**, *276*, 10737−10744.
(28) Schor, M.; Vreede, J.; Bolhuis, P. G. Elucidating the locking mechanism of peptides onto growing amyloid fibrils through transition path sampling. *Biophys. J.* **2012**, *103*, 1296−1304.
(29) Esler, W. P.; Stimson, E. R.; Jennings, J. M.; Vinters, H. V.; Ghilardi, J. R.; Lee, J. P.; Mantyh, P. W.; Maggio, J. E. Alzheimer's Disease Amyloid Propagation by a Template-Dependent Dock-Lock Mechanism. *Biochemistry* **2000**, *39*, 6288−6295.
(30) Gobbi, M.; Colombo, L.; Morbin, M.; Mazzoleni, G.; Accardo, E.; Vanoni, M.; Del Favero, E.; Cantù, L.; Kirschner, D. A.; Manzoni, C.; et al. Gerstmann-Sträussler-Scheinker disease amyloid protein polymerizes according to the "dock-and-lock" model. *J. Biol. Chem.* **2006**, *281*, 843−849.
(31) Cannon, M. J.; Williams, A. D.; Wetzel, R.; Myszka, D. G. Kinetic analysis of beta-amyloid fibril elongation. *Anal. Biochem.* **2004**, *328*, 67−75.
(32) Takeda, T.; Klimov, D. K. Dissociation of Aβ_{16-22} Amyloid Fibrils Probed by Molecular Dynamics. *J. Mol. Biol.* **2007**, *368*, 1202−1213.
(33) Reddy, G.; Straub, J. E.; Thirumalai, D. Dynamics of locking of peptides onto growing amyloid fibrils. *Proc. Natl. Acad. Sci. U. S. A.* **2009**, *106*, 11948−11953.

DOI: 10.1021/acs.jctc.9b00145
J. Chem. Theory Comput. 2019, 15, 3868−3874

(34) Nguyen, P. H.; Li, M. S.; Stock, G.; Straub, J. E.; Thirumalai, D. Monomer adds to preformed structured oligomers of Aβ-peptides by a two-stage dock-lock mechanism. *Proc. Natl. Acad. Sci. U. S. A.* **2007**, *104*, 111−116.
(35) Rosenman, D. J.; Connors, C. R.; Chen, W.; Wang, C.; García, A. E. Aβ monomers transiently sample oligomer and fibril-like configurations: Ensemble characterization using a combined MD/NMR approach. *J. Mol. Biol.* **2013**, *425*, 3338−3359.
(36) Lemkul, J. A.; Bevan, D. R. Assessing the stability of Alzheimer's amyloid protofibrils using molecular dynamics. *J. Phys. Chem. B* **2010**, *114*, 1652−1660.
(37) Rao Jampani, S.; Mahmoudinobar, F.; Su, Z.; Dias, C. L. Thermodynamics of Aβ16−21 dissociation from a fibril: Enthalpy, entropy, and volumetric properties. *Proteins: Struct., Funct., Genet.* **2015**, *83*, 1963−1972.
(38) Schwierz, N.; Frost, C. V.; Geissler, P. L.; Zacharias, M. Dynamics of Seeded Aβ40-Fibril Growth from Atomistic Molecular Dynamics Simulations: Kinetic Trapping and Reduced Water Mobility in the Locking Step. *J. Am. Chem. Soc.* **2016**, *138*, 527−539.
(39) Hess, B.; Kutzner, C.; van der Spoel, D.; Lindahl, E. GROMACS 4: Algorithms for Highly Efficient, Load-Balanced, and Scalable Molecular Simulation. *J. Chem. Theory Comput.* **2008**, *4*, 435−447.
(40) Colletier, J.; Laganowsky, A.; Landau, M.; Zhao, M.; Soriaga, A.; Goldschmidt, L.; Flot, D.; Cascio, D.; Sawaya, M. R.; Eisenberg, D. Molecular basis for amyloid-β polymorphism. *Proc. Natl. Acad. Sci. U. S. A.* **2011**, *108*, 16938−16943.
(41) Wiltzius, J. J.; Sievers, S. A.; Sawaya, M. R.; Cascio, D.; Popov, D.; Riekel, C.; Eisenberg, D. Atomic structure of the cross-beta spine of islet amyloid polypeptide (amylin). *Protein Sci.* **2008**, *17*, 1467−1474.
(42) Nelson, R.; Sawaya, M. R.; Balbirnie, M.; Madsen, A. O.; Riekel, C.; Grothe, R.; Eisenberg, D. Structure of the Cross-β Spine of Amyloid-Like Fibrils. *Nature* **2005**, *435*, 773−778.
(43) Lemkul, J. A.; Bevan, D. R. Assessing the Stability of Alzheimer's Amyloid Protofibrils Using Molecular Dynamics. *J. Phys. Chem. B* **2010**, *114*, 1652−1660.
(44) Šarić, A.; Chebaro, Y. C.; Knowles, T. P.; Frenkel, D. Crucial role of nonspecific interactions in amyloid nucleation. *Proc. Natl. Acad. Sci. U. S. A.* **2014**, *111*, 17869−17874.
(45) MacCallum, J. L.; Moghaddam, M. S.; Chan, H. S.; Tieleman, D. Hydrophobic Association of α-Helices, Steric Dewetting and Enthalpic Barriers to Protein Folding. *Proc. Natl. Acad. Sci. U. S. A.* **2007**, *104*, 6206−6210.
(46) Seibert, M. M.; Patriksson, A.; Hess, B.; Van Der Spoel, D. Reproducible polypeptide folding and structure prediction using molecular dynamics simulations. *J. Mol. Biol.* **2005**, *354*, 173−183.
(47) Kumar, S.; Rosenberg, J. M.; Bouzida, D.; Swendsen, R. H.; Kollman, P. A. The weighted histogram analysis method for free-energy calculations on biomolecules. I. The method. *J. Comput. Chem.* **1992**, *13*, 1011−1021.
(48) Dill, K. Dominant Forces in Protein Folding. *Biochemistry* **1990**, *29*, 7133−7155.
(49) Kauzmann, W. Some Factors in the Interpretation of Protein Denaturation. *Adv. Protein Chem.* **1959**, *14*, 1−63.
(50) Hawley, S. A. Reversible pressure-temperature denaturation of chymotrypsinogen. *Biochemistry* **1971**, *10*, 2436−2442.
(51) Privalov, P. L. Thermodynamics of Protein Folding. *J. Chem. Thermodyn.* **1997**, *29*, 447−474.
(52) Zipp, A.; Kauzmann, W. Pressure denaturation of metmyoglobin. *Biochemistry* **1973**, *12*, 4217−4228.
(53) Smeller, L. Pressure-Temperature Phase Diagrams of Biomolecules. *Biochim. Biophys. Acta, Protein Struct. Mol. Enzymol.* **2002**, *1595*, 11−29.
(54) Dias, C. L.; Ala-Nissila, T.; Wong-ekkabut, J.; Vattulainen, I.; Grant, M.; Karttunen, M. The Hydrophobic Effect and its Role in Cold Denaturation. *Cryobiology* **2010**, *60*, 91−99.
(55) Frank, H. S.; Evans, M. W. Free Volume and Entropy in Condensed Systems III. Entropy in Binary Liquid Mixtures; Partial Molal Entropy in Dilute Solutions; Structure and Thermodynamics in Aqueous Electrolytes. *J. Chem. Phys.* **1945**, *13*, 507.
(56) Narayanan, C.; Dias, C. L. Hydrophobic Interactions and Hydrogen Bonds in β-Sheet Formation. *J. Chem. Phys.* **2013**, *139*, 115103.
(57) Dias, C. L.; Hynninen, T.; Ala-Nissila, T.; Foster, A. S.; Karttunen, M. Hydrophobicity within the three-dimensional Mercedes-Benz model: Potential of mean force. *J. Chem. Phys.* **2011**, *134*, 065106.
(58) Robertson, A. D.; Murphy, K. P. Protein Structure and the Energetics of Protein Stability. *Chem. Rev.* **1997**, *97*, 1251−1268.
(59) Edsall, J. T. Apparent Molal Heat Capacities of Amino Acids and Other Organic Compounds. *J. Am. Chem. Soc.* **1935**, *57*, 1506−1507.
(60) Sedlmeier, F.; Netz, R. R. Solvation thermodynamics and heat capacity of polar and charged solutes in water. *J. Chem. Phys.* **2013**, *138*, 115101.
(61) Makhatadze, G.; Gill, S.; Privalov, P. Partial molar heat capacities of the side chains of some amino acid residues in aqueous solution: The influence of the neighboring charges. *Biophys. Chem.* **1990**, *38*, 33−37.
(62) Cabani, S.; Gianni, P.; Mollica, V.; Lepori, L. Group contributions to the thermodynamic properties of non-ionic organic solutes in dilute aqueous solution. *J. Solution Chem.* **1981**, *10*, 563−595.
(63) Ikenoue, T.; Lee, Y.-H.; Kardos, J.; Saiki, M.; Yagi, H.; Kawata, Y.; Goto, Y. Cold Denaturation of α-Synuclein Amyloid Fibrils. *Angew. Chem., Int. Ed.* **2014**, *53*, 7799−7804.
(64) Kim, H.-Y.; Cho, M.-K.; Riedel, D.; Fernandez, C. O.; Zweckstetter, M. Dissociation of Amyloid Fibrils of α-Synuclein in Supercooled Water. *Angew. Chem., Int. Ed.* **2008**, *47*, 5046−5048.
(65) Mishra, R.; Winter, R. Cold- and Pressure-Induced Dissociation of Protein Aggregation and Amyloid Fibrils. *Angew. Chem., Int. Ed.* **2008**, *47*, 6518.
(66) Sharp, K. Entropy-enthalpy compensation: Fact or artifact? *Protein Sci.* **2001**, *10*, 661−667.
(67) Thompson, M. J.; Sievers, S. A.; Karanicolas, J.; Ivanova, M. I.; Baker, D.; Eisenberg, D. The 3D profile method for identifying fibril-forming segments of proteins. *Proc. Natl. Acad. Sci. U. S. A.* **2006**, *103*, 4074−4078.
(68) Rizzi, L.; Auer, S. Amyloid Fibril Solubility. *J. Phys. Chem. B* **2015**, *119*, 14631−14636.
(69) Ricchiuto, P.; Brukhno, A. V.; Auer, S. Protein Aggregation: Kinetics versus Thermodynamics. *J. Phys. Chem. B* **2012**, *116*, 5384−5390.
(70) O'Brien, E. P.; Okamoto, Y.; Straub, J. E.; Brooks, B. R.; Thirumalai, D. Thermodynamic Perspective on the Dock-Lock Growth Mechanism of Amyloid Fibrils. *J. Phys. Chem. B* **2009**, *113*, 14421−14430.
(71) See the Supporting Information (SI).

DOI: 10.1021/acs.jctc.9b00145
J. Chem. Theory Comput. 2019, 15, 3868−3874